

QUENCH SIMULATION USING A RING-TYPE DEFECT MODEL

Yi Xie[†], Matthias Liepe and Hasan Padamsee

Cornell Laboratory for Accelerator-Based Sciences and Education (CLASSE),
Cornell University, Ithaca, NY 14853, USA

Abstract

A 2-dimensional ring-type defect thermal feedback model has been improved by including magnetic field enhancement at the pit edge. Latest simulation results show that there is a thermally stable state below the quench field with part of the edge becoming normal conducting, which can explain the preheating observed in thermometry measurements at fields below quench. 3D magnetic field enhancement calculations of pit structures were done using the Omega3P code to obtain realistic values for the magnetic field enhancement at typical pit dimensions.

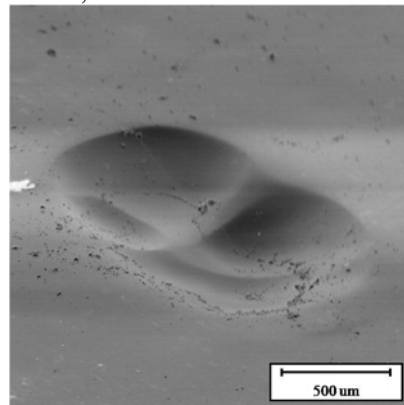


Figure 1: The SEM image of a pit causing quench at 120 mT in cavity LE1-HOR.

INTRODUCTION

Pit-like structures on the niobium surface of superconducting RF cavities have been shown to cause thermal breakdown under certain conditions. However, the field at which quench is caused by a pit defect varies significantly from pit to pit, and frequently, pits do not cause quench up to the maximum field obtained. Previous thermal feedback models treat pits as normal conducting disk-type or ring-type defects and aim to predict quench fields according to pit size [1],[2].

An interesting feature observed by temperature mapping at pit locations is that increased heating is found, starting well below the quench field [4]. Fig.1 shows a pit-like defect found in a single cell 1.5 GHz cavity which showed about 200mK pre-heating at the quench site just below the breakdown field of 120 mT. Since the thermometer efficiency is 20~25% [3], the actual outer wall temperature rise is 800~1000mK. Only part of this heating can be attributed to the typical high field Q-drop in BCP cavities without low temperature bake. Figure 2 shows two individual thermometer responses, one at the pit location, and one at a defect free area in the high magnetic field region. It shows that the defect heating has surpassed high-field Q slope above 80 mT. By subtracting the estimated Q slope heating, the pre-heating by the pit defect alone can be estimated. From this it is found that the temperature increase scale as H_{peak}^2 and is thus ohmic in nature [3].

In this paper we present an improved version of our ring defect model [2], which is not only able to predict the quench field caused by the pit, but also explains the presence of the pre-heating observed at fields below quench.

The key idea of this new pit model is that it includes the magnetic field enhancement at the pit edge.

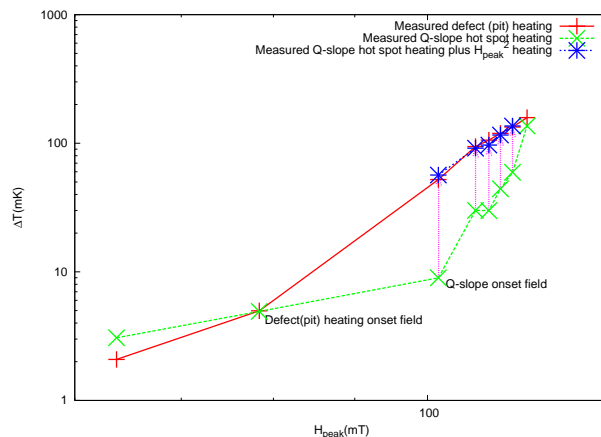


Figure 2: Individual thermometer response during test of cavity LE1-HOR. The blue symbols show the heating measured at the pit location, while the green symbols are from a location in the high magnetic field region showing the typical high field Q-drop in a BCP treated cavity.

IMPROVED RING-TYPE DEFECT MODEL

The phenomena of thermal magnetic breakdown has been numerically simulated over the years and is based on a thermal feedback process. Past models treated the defect as an axial-symmetric disk with its entire area becoming normal conducting when thermal breakdown happens. However, as observed in many cases, quench causing defects are correlated with pits on the surface with a sharp edge, and not disk like objects. Therefore, based on the assumption that only the edge of the pit becomes normal conducting, a 2-dimensional ring-type defect thermal program was

* Work supported by NSF CAREER award PHY-0841213 and Alfred P. Sloan Foundation
[†] yx39@cornell.edu

developed [2]. Figure 3 shows the mesh configuration difference between a ring-type defect and a disk-type defect. The ring-type defect model is based on the same heat balance equations and boundary conditions as the disk-defect thermal model [1].

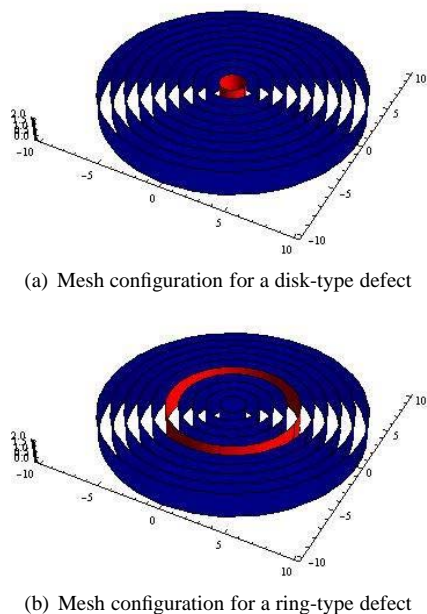


Figure 3: Different mesh distributions of ring-type and disk-type defect models with normal conducting (red) and superconducting (blue) mesh elements.

In the ring-type defect model, the program splits a cylindrical section of the niobium wall into many circular ring-shaped mesh elements. To model the heating at the edge of the pit, in the previous version of the ring defect model a normal conducting defect was located at a ring section at a certain distance from the center of the modeled niobium disk. To speed up simulations, the mesh density is higher near the defect element and lower away from it where temperature gradients are smaller. The mesh spacing in the radial direction was chosen to increase exponentially (the distance between the i -th element to the ring-defect is proportional to e^i). The z direction (through the niobium) can also be easily meshed using an exponential function. For a selected surface field at one side of the niobium disc, the RF power is calculated based on the temperature dependent surface resistance. Given the temperature dependent thermal conductivity of niobium and Kapitza conductance between niobium and helium, the RF power produced at the surface is compared with the power emitted into the helium bath at a given iteration number. The over-relaxation method is used to estimate the $(n + 1)$ -th iteration from n -th iteration. Once the two heat transfer numbers are sufficiently equal (e.g. their difference is less than 1.0×10^{-6}), thermal equilibrium is reached. The model is well calibrated and used to obtain quench field correlation with defect pit sizes. With

sufficient mesh densities, the model takes less than few minutes to converge.

The new feature added to the ring-type defect model discussed in this paper is a position dependent magnetic field enhancement (MFE) factor at the RF surface. For a first approximation, the enhancement factor is one far outside of the pit and jumps to a selected value above one at the pit edge. Inside the pit, the field enhancement factor is scaled below one because the surface magnetic field is lower compared with the field at the flat surface outside of a pit. Initially in the model, the entire surface is assumed to be superconducting. Only when the field exceeds the superheating (critical) magnetic field at the given temperature of the niobium at a given location, that section of the surface is assumed to be normal conducting.

Since an axis-symmetric mesh is used, a uniform MFE factor is assumed instead of angular dependent MFE factor along the pit edge.

Nevertheless, a 3-dimensional electromagnetic code is used to obtain realistic magnetic field enhancement factors based on measured surface pit dimensions.

HIGH PRECISION 3D SIMULATION OF MAGNETIC FIELD ENHANCEMENT

The magnetic field enhancement effect at the sharp edge/corner of a pit has been calculated in previous work [3],[6] [7]. The results obtained generally show a $r^{-1/3}$ dependence of magnetic field enhancement factor, where r is the radius of edge/corner. Real pit-like defects observed in the superconducting cavities have a complex 3-dimensional shape. To obtain a realistic field enhancement factor for these pits, we use SLAC's parallel computing EM code ACE3P [5] to compute the exact surface magnetic field in the entire pit edge area. Studies have shown that Omega3P has a very accurate surface field precision compared with other 3 dimensional codes [8]. As a first, simple example, we have simulated a rounded pit on the axis of a pillbox cavity with the TE_{111} mode. The size of modeled pit is small compared to the size of the cavity, which ensures that the surface field would be uniform over the area of the pit without the pit present. The pillbox cavity has a radius 100 mm, with a pit radius $R = 1$ mm. The simulated geometry and mesh configuration can be seen as Fig.4 and Fig.5.

The calculation was performed and checked with different mesh densities. As the pit edge radius r becomes smaller, the surface field results calculated by Omega3P becomes more dependent on the mesh densities. Nevertheless, for sufficiently dense meshes, our calculated results agree well with the $r^{-1/3}$ dependence of the maximum surface enhanced magnetic field. An example of the calculated surface magnetic field distribution is shown in Fig.6. The corresponding field enhancement factor near the edge of the pit is displayed in Fig.7. An angular non-uniform field enhancement around the edge can be seen from these results, with significant field enhancement in some sections.

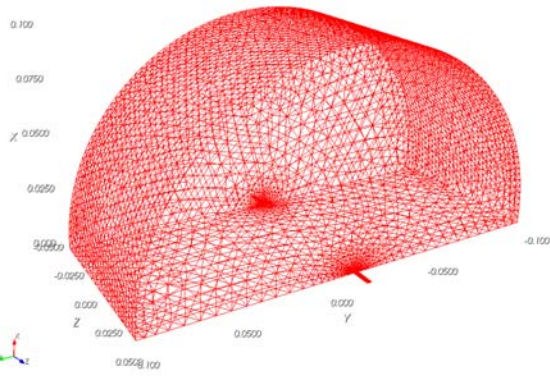


Figure 4: Geometry and mesh configuration used for the 3D pit MFE calculations.

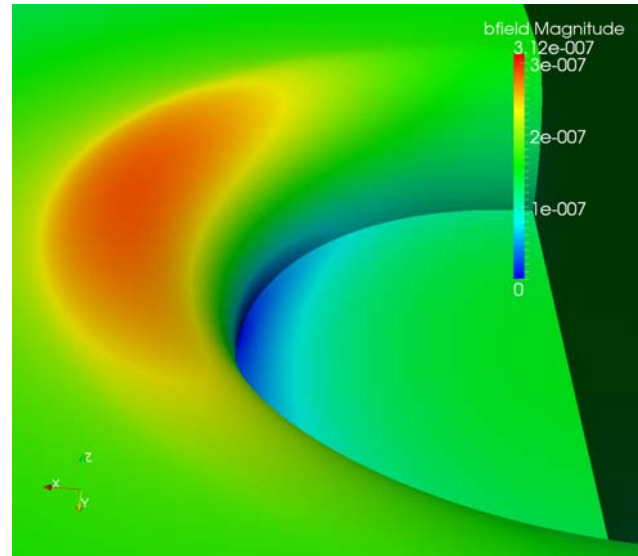


Figure 6: Magnetic field distribution near the pit edge.

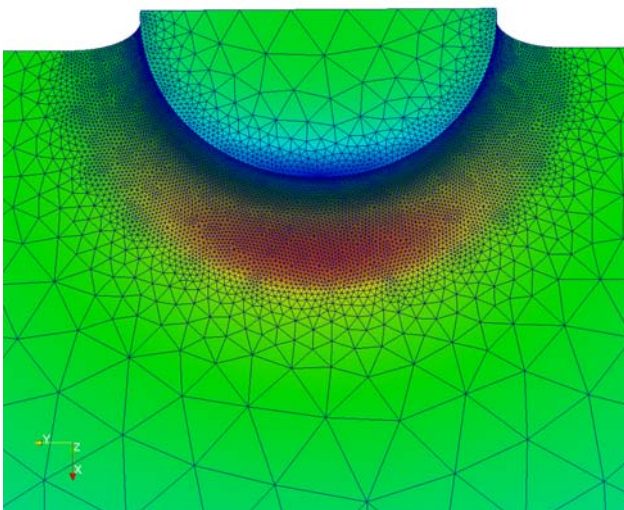


Figure 5: Mesh configuration at the pit used for 3D MFE calculations.

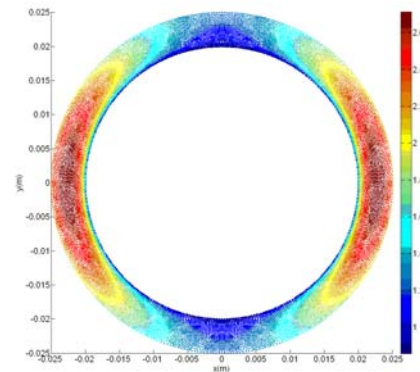


Figure 7: Magnetic field enhancement near the pit edge

RING-TYPE DEFECT MODEL RESULTS AND DISCUSSIONS

Simulations of ring-type defects of different radius and width (and thus different field enhancement factor at the pit) were performed to explore the relationship between the pit geometry and the quench field. Fig. 8 shows the temperature profile on the RF surface as function of radial distance from the center of the pit at a field just below quench. Clearly visible is the heating by the edge of the pit becoming normal conducting. The normal conducting resistance of niobium was taken as $10\text{m}\Omega$. Future versions of the ring defect model will also take into account the temperature dependence of the normal conducting resistance. Fig.9 shows a typical pre-quench temperature distribution at the cross section of the simulated heating by a pit. The RF field level

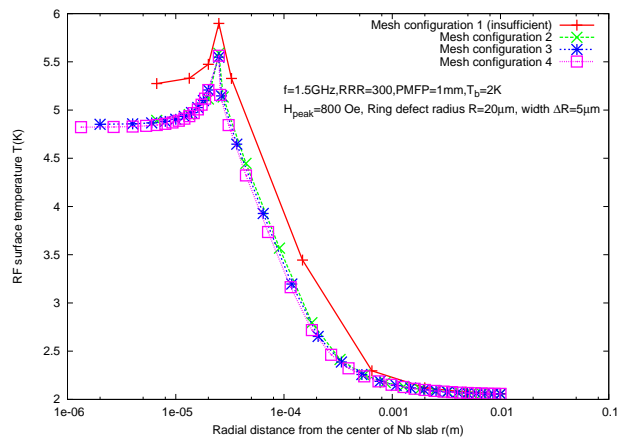


Figure 8: RF surface temperature distribution along the radial direction for a given ring-type defect.

is 1315 Oe which is slightly below the quench field of this pit defect of 1319 Oe. As can be seen from Fig.9, the highest temperature located at the pit edge is 5.76K. In contrast, the critical temperature of niobium at this field level is 5.4K. This confirms that the pit edge has become normal conducting, while the inside the pit the niobium remains superconducting. As the field raises, the normal conducting pit edge expands and finally leads to quench, when the entire simulated niobium slab becomes normal conducting. Using two different pit diameters with the same pit edge

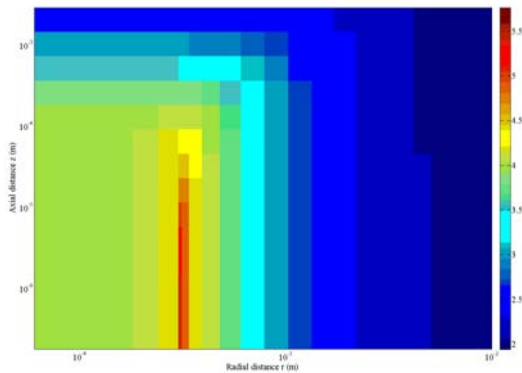


Figure 9: Temperature distribution at the cross section of the simulated niobium slab at a field level just below quench. The diameter of the simulated niobium disk is 10 mm with 3mm thickness. The field enhancement factor used at the edge of the pit corresponds to a pit of $30\ \mu\text{m}$ diameter with a edge radius of $1\ \mu\text{m}$. The RF field level is 1315 Oe which is slightly below the quench field of this pit defect of 1319 Oe. The helium bath temperature is 2K.

size, the quench fields were calculated by the improved ring-type model for different magnetic field enhancement factors as shown in Fig.10. In the blue color region, all parts of simulated niobium slab are superconducting. In the white region, at least the edge of the pit has become normal conducting. Notice that the pit edge becomes normal conducting at RF fields lower than the quench field, especially for larger field enhancement factors. This behavior provides an explanation for the heating observed at the location of a pit at fields below the quench field.

CONCLUSIONS

Simulations show that there is a thermally stable field region below the quench field for pit-like defects, at which only the edge of the pit is normal conducting. The existence of this stable normal conducting region can explain the pre-heating (and maybe Q-slope reduction found before quench) observed in thermometry results. As shown before [1], these pre-heating signals can give clues of the size of the pits. Currently, efforts are being made to extend this model into 3 dimension so that the full spacial dependence of the magnetic field enhancement factor can be included.

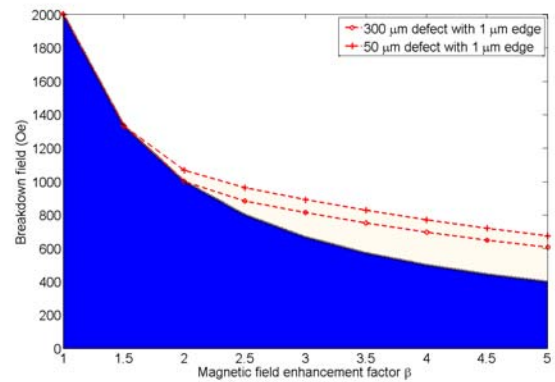


Figure 10: Quench fields v.s. difference ring-type defect sizes for different magnetic field enhancement factors. In the blue color region, all parts of simulated niobium slab are superconducting. In the white region, at least the edge of the pit has become normal conducting.

REFERENCES

- [1] Y. Xie, Hasan Padamsee, Alexander Romanenko, "Relationship Between Defects Pre-Heating and Defects Size" SRF2009, Berlin, Germany.
- [2] Yi Xie, Matthias Liepe, Hasan Padamsee, "THERMAL MODELING OF RING-TYPE DEFECTS", SRF2009, Berlin, Germany.
- [3] J. Knobloch, PhD thesis, Cornell University, 1997.
- [4] Q. S. Shu, et.al., "Experimental Investigation of Quenches in Superfluid He of TESLA 9-Cell Superconducting Cavities" SRF1995, Gif-sur-Yvette, France.
- [5] Lie-Quan Lee, Zenghai Li, Cho Ng, and Kwok Ko, Tech. Rep., SLAC-PUB-13529, 2009, "Omega3P: A Parallel finite-Element Eigenmode Analysis Code for Accelerator Cavities"
- [6] Y. Iwashita, "Evaluation of Magnetic Field Enhancement Along a Boundary", Linac04, Lubeck, Germany.
- [7] V. Shemelin, H. Padamsee, "Magnetic field enhancement at pits and bumps on the surface of superconducting cavities" SRF Report 080903-04, Cornell University.
- [8] K. Tian et.al., "BENCHMARK OF DIFFERENT ELECTROMAGNETIC CODES FOR THE HIGH FREQUENCY CALCULATION", PAC09, Vancouver, Canada